Collective Buckling of a Two-Dimensional Array of Nanoscale Columns

Ziguang Chen, Jiashi Yang, and Li Tan*

Department of Engineering Mechanics and Nebraska Center for Materials and Nanoscience, University of Nebraska, Lincoln, Nebraska 68588-0526

Received: May 26, 2008; Revised Manuscript Received: September 22, 2008

Periodic soft nanostructures are building blocks for small devices. However, mechanical failure in the form of structure buckling or distortion from their original shape is often reported when the dimension of these soft structures were reduced to below submicron scale. Such a phenomenon seriously limits a reliable impact of these nanostructures to greater applications. Current understandings of buckling of soft 2-D nanostructures are limited. The substrate for these soft nanostructures is usually very compliant. Neighboring nanostructures could interact through the deformation of the substrate. We analyze the collective buckling of a two-dimensional array of nanoscale columns with their lower ends built into an elastic substrate. Buckling of these nanostructures is mathematically described by an eigenvalue problem. Numerical analyses show patterned collapse for these 2-D nanostructures, qualitatively matching reported experimental findings. Our efforts are useful toward the understanding and manufacturing of many two-dimensional nanoscale features.

Introduction

Two-dimensional (2-D) column arrays composed of elastic materials have attracted increasing attention in the nanotechnology community for many applications, including dynamic tuning of surface wetting, dry adhesives that mimic gecko foot fibrillars, efficient microneedles in drug delivery, substrates for sensing cell response and MEMS actuators.[1−5] Although properties of these elastic structures can be further enriched by additional functionality like thermo-, electro-, or magneto-responsive features, mechanical instability or buckling was revealed, particularly when the dimension of the soft structures was reduced to below submicron scale.[6−11] One of the most common instabilities, for instance, is structure buckling. Such a phenomenon was experimentally reported, where two neighboring beams in an array would lean toward each other.[12] Because structure buckling affects a reliable application of the nanoscale features and buckling of soft nanostructures has certain aspects that are unique and are different from conventional macroscopic structures, it is of current research interest.

The substrate for these periodic soft nanostructures is usually very compliant. Neighboring nanostructures could interact through the deformation of the substrate. The results from the buckling analysis in conventional macroscopic structures are usually for a single beam.[13] Some of those results are relevant to the buckling of the above featured structures, e.g., the buckling of a beam under its own weight;[13] the buckling of a beam lying on an elastic foundation;[13] and the lateral torsional buckling of a high beam.[14] For periodic soft nanostructures, there are brief theoretical results on the buckling of a single beam-like structure without elastic interaction with the substrate by direct application of the results from structural engineering. In a relatively recent analysis,[15,16] the buckling of a single beam and the contact of two buckled beams were studied for the soft lithography process.

In the nanostructures we are considering, the columns and the substrate are of the same deformable material. However, in the existing analyses[15,16] the substrate was treated as rigid. The deformation of the substrate and the beam interaction through the substrate were not considered. Therefore their results can only provide understanding of the buckling of a single beam but cannot describe the collective buckling of interacting beams.

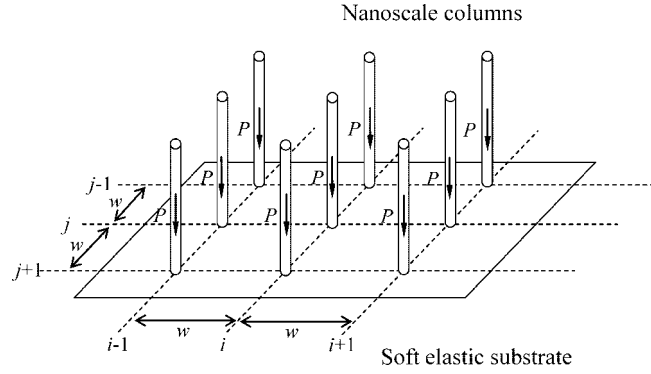

Figure 1. Two-dimensional array of rigid nanoscale columns on an elastic substrate.

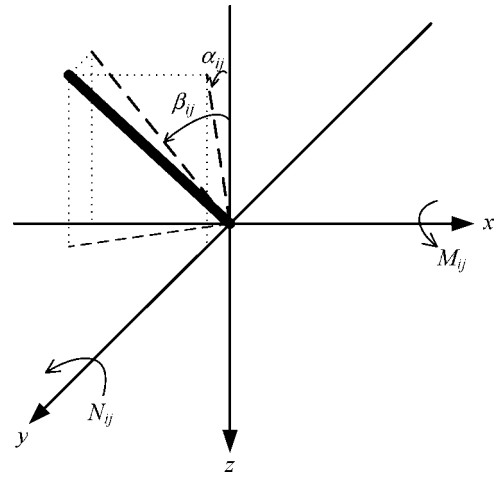

Figure 2. Notation for rotations and couples.

* Corresponding author (ltan4@unl.edu, Fax 402-472-8292, Tel. 402-472-4018).

10.1021/jp8046399 CCC: $40.75
Published on Web 10/31/2008

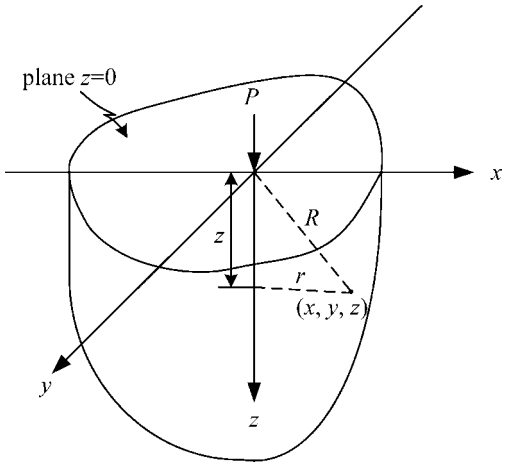

Figure 3. Elastic half-space with a concentrated surface normal force.

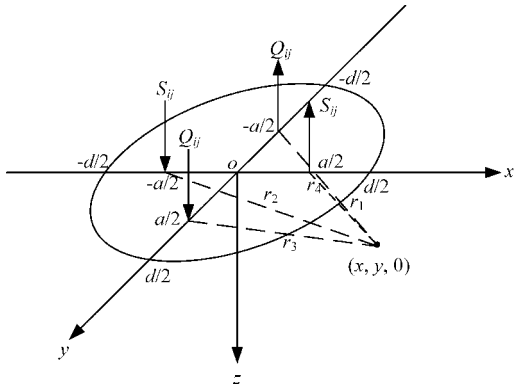

Figure 4. Bottom area of a beam on the surface of the half-space.

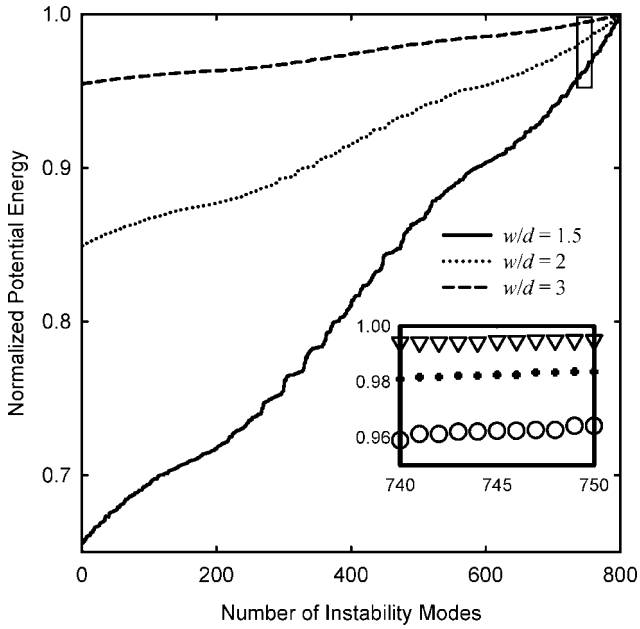

Figure 5. Normalized potential energy versus various instability modes.

A recent major progress in the buckling analysis of one-dimensional (1-D) soft nanostructures was made in our recent work.[9,17] Due to the inclusion of the most basic effect, i.e., neighboring nanostructures can interact through the deformation of the substrate, our model was able to describe the collective buckling of many beams and lead to results qualitatively

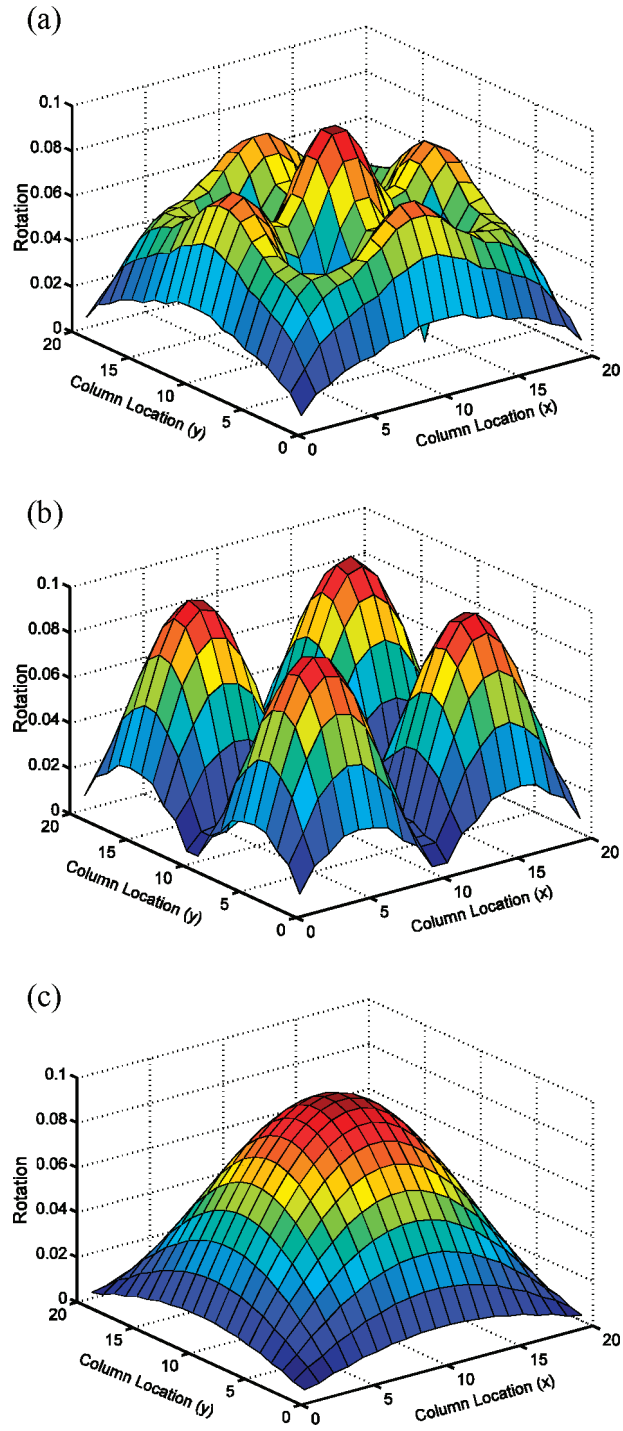

Figure 6. Three different modes of collective buckling among 20 × 20 columns: (a) mode #8 and (b) mode #10 occur at a higher energy level, and (c) mode #1 appears with the lowest potential energy.

matching experimental findings. Although they are adequate to convey the concept of collective buckling of a 1-D array, buckling analysis based upon 2-D array of nanostructures was never reported. We present the analysis in this article to fill such a gap.

Results and Discussion

1. Analytical Model for Collective Buckling in 2-D Arrays. Our theoretical model consists of many identical, uniformly spaced, rigid beams on an elastic substrate (see Figure 1). We focus on the collective buckling of beams on a deformable

substrate. The most important mechanism is the interaction through the deformation of the substrate. To make the problem simple and yet show the most basic physics, we treat the substrate as deformable but the columns as rigid.[9] Buckling of these rigid beams is described by deviation from their vertical positions (tilting). The weight of a beam is represented by a vertical force P acting at the center of the beam. There may be other causes for buckling and weight is just one of them. Other possible causes are residual stress due to the thermal processes in manufacturing and shrinkage in solidification, etc. In this paper we follow ref 15 and study the effect of gravity only. For a circular beam $P = \rho g \pi d^2 h/4$, where d is the diameter of the cross section of the beams. As in ref 9 we neglect the vertical and horizontal displacements of the bottoms of the beams and focus on the major deformation, i.e., the tilting of the beams during buckling. For the most basic behavior of buckling it is sufficient to consider small tilting of the beams and infinitesimal deformations of the substrate. Then an arbitrary tilting can be decomposed into the sum of two small tiltings about the x and y axes. For a typical beam labeled by (i,j), let the tiltings around the x and y axes be α_{ij} and β_{ij}, respectively (see Figure 2). When a beam tilts, the beam bottom interacts with the substrate through two couples (moments) around the x and y axes. They are denoted by M_{ij} and N_{ij}, respectively and their positive directions are shown in Figure 2. These moments are resultants of distributed normal stresses at the bottom cross section of the beam. Mathematically, they are given by

$$M = \int_A \sigma_z y \, dA \qquad N = -\int_A \sigma_z x \, dA \tag{1}$$

where A is the beam bottom cross section and σ_z is the normal stress there.

The tiling angle α_{ij} (or β_{ij}) at location (i,j) is due to the moments M_{mn} and N_{mn} at all locations (m, n). Within the linear theory of elasticity, by superposition, we can write

$$\begin{aligned}\alpha_{ij} = &\sum_{m=1}^{\infty}\sum_{n=1}^{\infty} A_{ij;mn} M_{mn} + \\ &\sum_{m=1}^{\infty}\sum_{n=1}^{\infty} B_{ij;mn} N_{mn} \cong \sum_{m=-1}^{1}\sum_{n=-1}^{1} A_{ij;(i+m)(j+n)} M_{mn} + \\ &\sum_{m=-1}^{1}\sum_{n=-1}^{1} B_{ij;(i+m)(j+n)} N_{mn}\, \beta_{ij} = \sum_{m=1}^{\infty}\sum_{n=1}^{\infty} C_{ij;mn} M_{mn} + \\ &\sum_{m=1}^{\infty}\sum_{n=1}^{\infty} D_{ij;mn} N_{mn} \cong \sum_{m=-1}^{1}\sum_{n=-1}^{1} C_{ij;(i+m)(j+n)} M_{mn} + \\ &\sum_{m=-1}^{1}\sum_{n=-1}^{1} D_{ij;(i+m)(j+n)} N_{mn}\end{aligned} \tag{2}$$

where the interaction (or influence) coefficients $A_{ij;mn}$, $B_{ij;mn}$, $C_{ij;mn}$ and $D_{ij;mn}$ physically represent the tiltings at one location due to couples acting at another (or the same) location. These coefficients can be calculated from the theory of elasticity and are given in the following section. In eq 2 the approximation of nearest-neighbor interaction is made. The tilting at one location is due to the couples at the nearest eight locations. Equation 2 can be inverted to give

$$\begin{aligned}M_{ij} = &\sum_{m=1}^{\infty}\sum_{n=1}^{\infty} a_{ij;mn}\alpha_{mn} + \\ &\sum_{m=1}^{\infty}\sum_{n=1}^{\infty} b_{ij;mn}\beta_{mn} \cong \sum_{m=-1}^{1}\sum_{n=-1}^{1} a_{ij;(i+m)(j+n)}\alpha_{mn} + \\ &\sum_{m=-1}^{1}\sum_{n=-1}^{1} b_{ij;(i+m)(j+n)}\beta_{mn}\, N_{ij} = \sum_{m=1}^{\infty}\sum_{n=1}^{\infty} c_{ij;mn}\alpha_{mn} + \\ &\sum_{m=1}^{\infty}\sum_{n=1}^{\infty} d_{ij;mn}\beta_{mn} \cong \sum_{m=-1}^{1}\sum_{n=-1}^{1} c_{ij;(i+m)(j+n)}\alpha_{mn} + \\ &\sum_{m=-1}^{1}\sum_{n=-1}^{1} d_{ij;(i+m)(j+n)}\beta_{mn}\end{aligned} \tag{3}$$

which are expressions for the moments at a typical location due to tiltings at other locations. For a typical beam, the moment equilibrium equations about the x and y axes are

$$\begin{aligned}&\frac{\alpha_{ij} hP}{2} - \sum_{m=-1}^{1}\sum_{n=-1}^{1} a_{ij;(i+m)(j+n)}\alpha_{mn} - \\ &\qquad \sum_{m=-1}^{1}\sum_{n=-1}^{1} b_{ij;(i+m)(j+n)}\beta_{mn} = 0 \\ &\frac{\beta_{ij} hP}{2} - \sum_{m=-1}^{1}\sum_{n=-1}^{1} c_{ij;(i+m)(j+n)}\alpha_{mn} - \sum_{m=-1}^{1}\sum_{n=-1}^{1} d_{ij;(i+m)(j+n)}\beta_{mn} = 0\end{aligned} \tag{4}$$

Equation 4 is a system of homogeneous, linear equations. The trivial solution with all tiltings equal to zero is the unbuckled state. We are interested in nontrivial solutions representing buckled states. Then mathematically eq 4 is an eigenvalue problem. We look for values of Ph for which nontrivial solutions exist. The eigenvectors determine the buckled states of the structure.

2. Determination of Interaction Coefficients. First we summarize the basic results of the solution to the elasticity problem (the Boussinesq problem) of a half-space with a concentrated normal force (see Figure 3). This will be needed in the determination of the interaction coefficients. The displacement fields in cylindrical coordinates are[18]

$$\begin{aligned}u_r &= \frac{(1-2\nu)(1+\nu)P}{2\pi E r}\left[z(r^2+z^2)^{-1/2} - 1 + \frac{1}{(1-2\nu)} r^2 z (r^2+z^2)^{-3/2}\right] \\ w &= \frac{P}{2\pi E}[(1+\nu)z^2(r^2+z^2)^{-3/2} + 2(1-\nu^2)(r^2+z^2)^{-1/2}]\end{aligned} \tag{5}$$

where E is the Young's modulus and ν is the Poisson's ratio. In particular, for the boundary plane ($z = 0$), the displacements are

$$(u_r)_{z=0} = -\frac{(1-2\nu)(1+\nu)P}{2\pi E r} \qquad (w)_{z=0} = \frac{P(1-\nu^2)}{\pi E r} \tag{6}$$

Next, we consider the tilting angles and the couples at the bottom of a beam with a circular cross section with a diameter

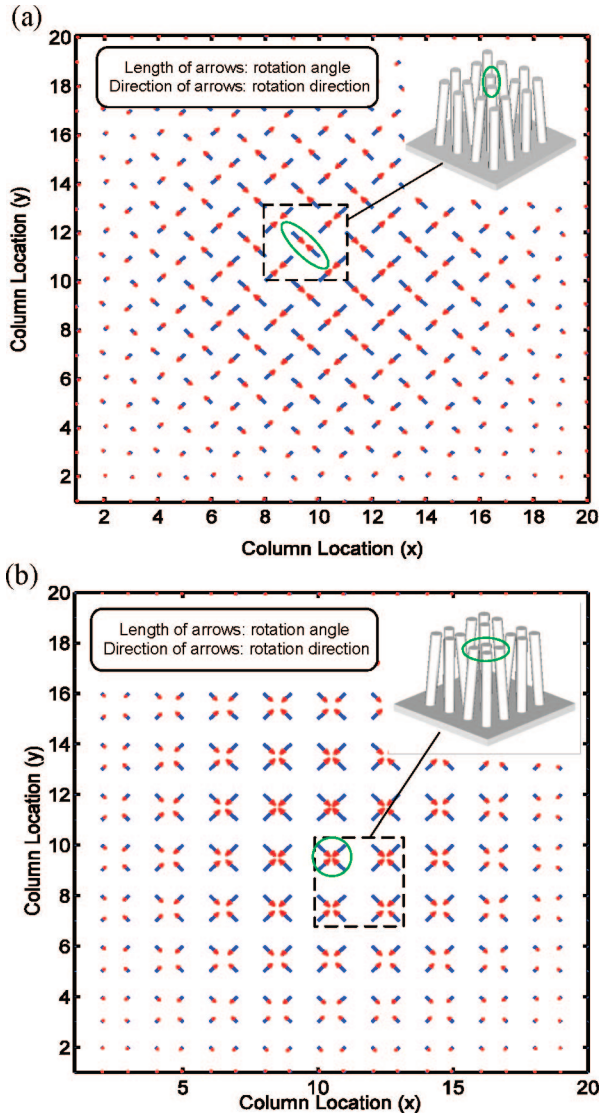

Figure 7. Two different modes with the same distribution of rotation magnitudes: (a) the first mode #1 and (b) the last mode #800.

d (see Figure 4). For the moments about the x and y axes, which are resultants of distributed forces, as an approximation, we consider the moments to be due to two pairs of concentrated forces Q_{ij} and S_{ij}, respectively, acting at the centroids of the corresponding semicircular areas, with $a = 4d/(3\pi)$. Then we can obtain the displacement field in the substrate under the four concentrated forces by superposition of the Boussinesq solution. With the displacement field known, we then calculate the deformation at the beam bottom and thus determine the tilting angles of the beam. Specifically, we first find the vertical displacements of two points at $x = \pm d/2$ and $y = 0$ in the bottom cross-section of the beam (and similarly those at $y = \pm d/2$ and $x = 0$). The difference of the vertical displacements of these two points when divided by the distance d between them gives a measure of the tilting. For example

$$\alpha = \frac{w(x=0,y=d/2,z=0) - w(x=0,y=-d/2,z=0)}{d} \quad (7)$$

Similarly, in general, the interaction coefficients are

$$A_{ij;ij} = D_{ij;ij} = \frac{(1-\nu^2)}{\pi E a d}\left[\left(\frac{d}{2}-\frac{a}{2}\right)^{-1} - \left(\frac{d}{2}+\frac{a}{2}\right)^{-1} - \left(\frac{d}{2}+\frac{a}{2}\right)^{-1} + \left(\frac{d}{2}-\frac{a}{2}\right)^{-1}\right] B_{ij;ij} = C_{ij;ij} = 0 \quad (8)$$

$$A_{ij;(i-1)(j-1)} = D_{ij;(i-1)(j-1)} = A_{ij;i(j+1)} = D_{ij;(i+1)j} = \frac{(1-\nu^2)}{\pi E a d}\left[\left(w-\frac{d}{2}+\frac{a}{2}\right)^{-1} - \left(w-\frac{d}{2}-\frac{a}{2}\right)^{-1} - \left(w+\frac{d}{2}+\frac{a}{2}\right)^{-1} + \left(w+\frac{d}{2}-\frac{a}{2}\right)^{-1}\right]$$
$$B_{ij;i(j-1)} = C_{ij;(i-1)j} = B_{ij;i(j+1)} = C_{ij;(i+1)j} = 0 \quad (9)$$

$$A_{ij;(i-1)(j-1)} = D_{ij;(i-1)(j-1)} = A_{ij;(i+1)(j+1)} = D_{ij;(i+1)(j+1)} = \frac{(1-\nu^2)}{\pi E a d}\left\{\left[w^2+\left(w-\frac{d}{2}+\frac{a}{2}\right)^2\right]^{-1/2} - \left[w^2+\left(w-\frac{d}{2}-\frac{a}{2}\right)^{-2}\right]^{-1/2} - \left[w^2+\left(w+\frac{d}{2}+\frac{a}{2}\right)^2\right]^{-1/2} + \left[w^2+\left(w+\frac{d}{2}-\frac{a}{2}\right)^2\right]^{-1/2}\right\}$$
$$B_{ij;(i-1)(j-1)} = C_{ij;(i-1)(j-1)} = B_{ij;(i+1)(j+1)} = C_{ij;(i+1)(j+1)} = \frac{(1-\nu^2)}{\pi E a d}\left\{\left[\left(w-\frac{a}{2}\right)^2+\left(w-\frac{d}{2}\right)^2\right]^{-1/2} - \left[\left(w+\frac{a}{2}\right)^2+\left(w-\frac{d}{2}\right)^2\right]^{-1/2} - \left[\left(w-\frac{a}{2}\right)^2+\left(w+\frac{d}{2}\right)^2\right]^{-1/2} + \left[\left(w+\frac{a}{2}\right)^2+\left(w+\frac{d}{2}\right)^2\right]^{-1/2}\right\} \quad (10)$$

$$A_{ij;(i-1)j} = D_{ij;i(j-1)} = A_{ij;(i+1)j} = D_{ij;i(j+1)} = \frac{(1-\nu^2)}{\pi E a d}\left\{\left[w^2+\left(-\frac{d}{2}+\frac{a}{2}\right)^2\right]^{-1/2} - \left[w^2+\left(\frac{d}{2}+\frac{a}{2}\right)^2\right]^{-1/2} - \left[w^2+\left(\frac{d}{2}+\frac{a}{2}\right)^2\right]^{-1/2} + \left[w^2+\left(\frac{d}{2}-\frac{a}{2}\right)^2\right]^{-1/2}\right\},$$
$$B_{ij;(i-1)j} = C_{ij;i(j-1)} = B_{ij;(i+1)j} = C_{ij;i(j+1)} = 0 \quad (11)$$

$$A_{ij;(i-1)(j+1)} = D_{ij;(i+1)(j-1)} = A_{ij;(i+1)(j-1)} = D_{ij;(i-1)(j+1)} = \frac{(1-\nu^2)}{\pi E a d}\left\{\left[w^2+\left(w+\frac{d}{2}-\frac{a}{2}\right)^2\right]^{-1/2} - \left[w^2+\left(w+\frac{d}{2}+\frac{a}{2}\right)^2\right]^{-1/2} - \left[w^2+\left(w-\frac{d}{2}-\frac{a}{2}\right)^2\right]^{-1/2} + \left[w^2+\left(w-\frac{d}{2}+\frac{a}{2}\right)^2\right]^{-1/2}\right\}$$
$$B_{ij;(i-1)(j+1)} = C_{ij;(i+1)(j-1)} = B_{ij;(i+1)(j-1)} = C_{ij;(i-1)(j+1)} = \frac{(1-\nu^2)}{\pi E a d}\left\{\left[\left(w-\frac{a}{2}\right)^2+\left(w+\frac{d}{2}\right)^2\right]^{-1/2} - \left[\left(w+\frac{a}{2}\right)^2+\left(w+\frac{d}{2}\right)^2\right]^{-1/2} - \left[\left(w-\frac{a}{2}\right)^2+\left(w-\frac{d}{2}\right)^2\right]^{-1/2} + \left[\left(w+\frac{a}{2}\right)^2+\left(w-\frac{d}{2}\right)^2\right]^{-1/2}\right\} \quad (12)$$

3. Numerical Results and Discussion. Equation 4 is an algebraic eigenvalue problem with a large number of equations. Therefore simple analytical results are not possible and the equations need to be solved numerically. As an example, we consider a 2-D array with 20 × 20 nanoscale columns. For this 20 × 20 2-D array, 800 values of $Ph/2$ representing different collective buckling modes are obtained from eq 4. When

buckling occurs, the loss of gravity potential is equal to the increase of strain energy. This energy criterion was established by Timoshenko in ref 13. Therefore potential energy at each instability modes can be calculated through either strain energy or gravity energy. For the kth instability mode, the strain energy from the substrate is calculated by formula

$$U^k = \sum_{j=1}^{20} \sum_{i=1}^{20} U_{ij}^k \tag{13}$$

where $U_{ij}^k = {}^1/_2 M_{ij}^k \alpha_{ij}^k + {}^1/_2 N_{ij}^k \beta_{ij}^k$. Because $M_{ij}^k = (Ph/2)^k \alpha_{ij}^k$ and $N_{ij}^k = (Ph/2)^k \beta_{ij}^k$, where $(Ph/2)^k$represents the eigenvalue at the kth mode, eq 13 can be written as

$$U^k = (Ph/2)^k \sum_{j=1}^{20} \sum_{i=1}^{20} [(\alpha_{ij}^k)^2 + (\beta_{ij}^k)^2] = (Ph/2)^k \sum_{j=1}^{20} \sum_{i=1}^{20} (\phi_{ij}^k)^2 \tag{14}$$

where φ_{ij}^k represents the magnitude of the rotation angle of the ijth column at the kth mode. The calculated strain energy, or potential energy, is then normalized and plotted as shown in Figure 5. Clearly, the potential energy of each individual mode of collective buckling for this 20 × 20 2-D array varies rather substantially. In this figure, we consider the influence of column spacing to the potential energy, where three different ratios of spacing over diameter (w/d) are used. Generally, the smaller the spacing/diameter ratio, the lower the potential energy will be. Because a lower potential energy always indicates a relative easiness of buckling, decreasing the spacing of this 2-D array will increase the possibility of collective buckling.

Furthermore, the 800 modes of collective buckling can be reduced to 400 due to the symmetry of the 2-D array. To highlight a few, we selected three different types of buckling modes and plotted the corresponding rotation magnitudes of the columns and illustrated the collective buckling in Figure 6. These three modes represent two frequently seen instabilities in nanomanufactured 2-D array (Figures 6a,b),[1,19] and one rarely observed mode (Figure 6c).[12] Generally, a periodic pattern of buckling is clearly visible for all these modes, with the first two occurring at much higher potential energy and the third one at the lowest energy level. In Figures 6a,b, buckled nanoscale columns are grouped into different patterns, where four similar patterns are shown in Figure 6b and one centering mode appears in addition to these in Figure 6a. Note that some buckled states can shear similar distribution of rotation magnitudes. Taking the first mode (#1 in Figure 5) and the last mode (#800 in Figure 5) as an example, although same distribution of rotation magnitudes (Figure 6c) exists at these two modes, the buckled states based on their rotation angles and directions, showed in Figure 7, are different. Figure 7a shows the mode with a herringbone feature, where two neighboring columns lean toward each other, whereas at the mode with the highest potential energy, every four columns lean together. Even though the lowest mode depicts the most possible way of collective buckling, control of the external impact to the least amount of energy usually requires a delicate balance. For instance, when the adhesions between the soft columns are suppressed, experimental results in ref 12 do match with our theoretical calculations. It is worthwhile to note that the present analysis simply treats elastic beams as rigid ones and make an assumption the bottoms of the beams can rotate but cannot move horizontally or vertically. These approximations make the system over stiff, for in real situations the beams are elastic and can bend, and the bottoms of the beams can move in both horizontal and vertical directions. However, our earlier efforts[17] found influences of these two approximations will not affect the collective buckling modes significantly and our presented results can be reliable snapshots of all the possible buckling modes in reality. And a superposition of all these basic modes should lead to a full picture of 2-D buckling in nanostructuring, the results obtained hence represent a significant progress beyond all previous work.

Summary

One of the most prominent features for periodic soft nanostructures is their role as building blocks for small devices. Comparing to their rigid counterparts, assembled devices have a few unique merits, like light weight, flexible mechanical deformation, and cost-effective manufacturing. However, mechanical failure in the form of structure buckling or distortion from their original shape is often reported when the dimensions of these soft structures were reduced to below submicron scale. Such a phenomenon seriously limits a reliable impact of these nanostructures to greater applications. Current understanding of the buckling of these structures is rather limited. By considering the interactions between closely packed nanostructures, buckling modes that are more accurate and more complete than before are predicted. A mechanics model is constructed and used in the theoretical analysis of a two-dimensional array of interacting columns. According to the model, buckling of the structure is mathematically described by an eigenvalue problem. The spacing between the columns will affect the collective buckling. Different buckled patterns can be obtained by controlling the geometry of these nanoscale columns. The results obtained represent a significant progress from our previous work.

Acknowledgment. The project described above is made possible by Nebraska Tobacco Settlement Biomedical Research Development Fund, Charles J. Millard Trust Fund, NSF EPSCoR and NSF MRSEC.

References and Notes

(1) Geim, A. K.; Dubonos, S. V.; Grigorieva, I. V.; Novoselov, K. S.; Zhukov, A. A.; Shapoval, S. Y. *Nat. Mater.* **2003**, *2*, 461–463.

(2) Kim, K.; Park, S.; Lee, J. B.; Manohara, H.; Desta, Y.; Murpphy, M.; Ahn, C. *Microsyst. Technol.* **2002**, *9*, 5.

(3) McAllister, D. V.; Wang, P. M.; Davis, S. P.; Park, J. H.; Canatella, P. J.; Allen, M. G.; Prausnitz, M. R. *Proc. Natl. Acad. Sci. U.S.A.* **2003**, *100*, 13755–13760.

(4) Nomura, S.; Kojima, H.; Ohyabu, Y.; Kuwabara, K.; Miyauchi, A.; Uemura, T. *Jpn. J. Appl. Phys.* **2005**, *44*, L1184–L1186.

(5) Zhang, L.; Zhou, Z. L.; Cheng, B.; DeSimone, J. M.; Samulski, E. T. *Langmuir* **2006**, *22*, 8576–8580.

(6) Chuang, W. C.; Ho, C. T.; Wang, W. C. *Opt. Express* **2005**, *13*, 6685–6692.

(7) Delamarche, E.; Schmid, H.; Michel, B.; Biebuyck, H. *Adv. Mater.* **1997**, *9*, 741–746.

(8) Evans, B. A.; Shields, A. R.; Carroll, R. L.; Washburn, S.; Falvo, M. R.; Superfine, R. *Nano Lett.* **2007**, *7*, 1428–1434.

(9) Lin, H. J.; Yang, J. S.; Tan, L.; Xu, J.; Li, Z. *J. Phys. Chem. C* **2007**, *111*, 13348–13356.

(10) Schmid, H.; Michel, B. *Macromolecules* **2000**, *33*, 3042–3049.

(11) Xia, Y. N.; Whitesides, G. M. *Annu. Rev. Mater. Sci.* **1998**, *28*, 153–184.

(12) Zhang, Y.; Lo, C. W.; Taylor, J. A.; Yang, S. *Langmuir* **2006**, *22*, 8595–8601.

(13) Timoshenko, S. P. *Theory of Elastic Stability*; McGraw-Hill: New York, 1936.

(14) Alfutov, N. A. *Stability of Elastic Structures*; Springer: Berlin, Germany, 2000.

(15) Hui, C. Y.; Jagota, A.; Lin, Y. Y.; Kramer, E. J. *Langmuir* **2002**, *18*, 1394–1407.

(16) Sharp, K. G.; Blackman, G. S.; Glassmaker, N. J.; Jagota, A.; Hui, C. Y. *Langmuir* **2004**, *20*, 6430–6438.

(17) Lin, H. J.; Chen, Z. G.; Yang, J. S.; Tan, L. To be submitted.

(18) Timoshenko, S. P.; Goodier, J. N. *Theory of Elasticity*, 3rd ed.; McGraw-Hill: New York, 1970.

(19) Wang, C. L.; Jia, G. Y.; Taherabadi, L. H.; Madou, M. J. *J. Microelectromech. Syst.* **2005**, *14*, 348–358.

JP8046399